

Supporting Information

Bimetallic Au-Ag on Patterned Substrate derived from Discarded Blu-ray discs: Simple, Inexpensive, Stable and Reproducible SERS Substrates

*Aroonsri Ngamaroonchote, Kullavadee Karn-orachai**

National Nanotechnology Center (NANOTEC), National Science and Technology Development Agency (NSTDA), Pathum Thani 12120, Thailand

* Corresponding author. Tel.: +66 2 564 7100

E-mail address: kullavadee.kar@nanotec.or.th

Optimization of r-AgBD-ROM substrate fabrication

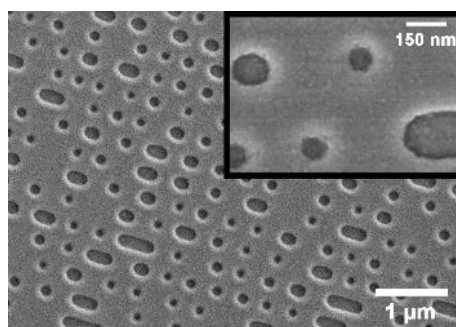


Figure S1. FE-SEM images of AgBD-ROM. Insert is an enlarged image.

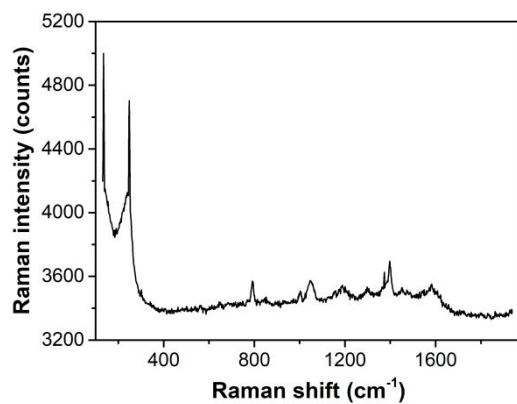


Figure S2. Raman spectra background of r-AgBD-ROM.

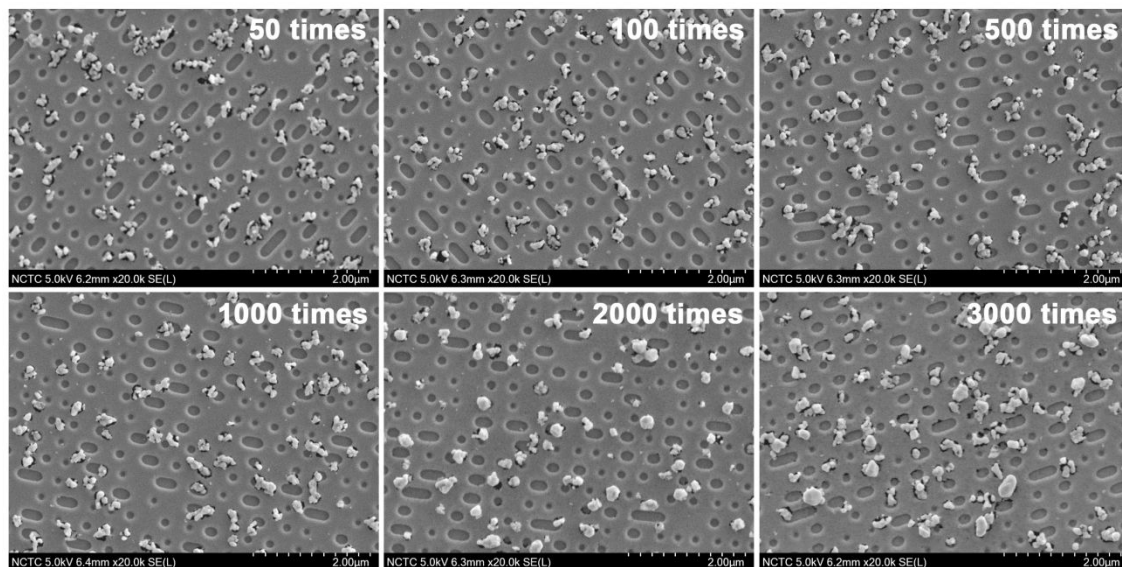


Figure S3. FE-SEM images of r-AgBD-ROM fabricated under different the number of step-scan.

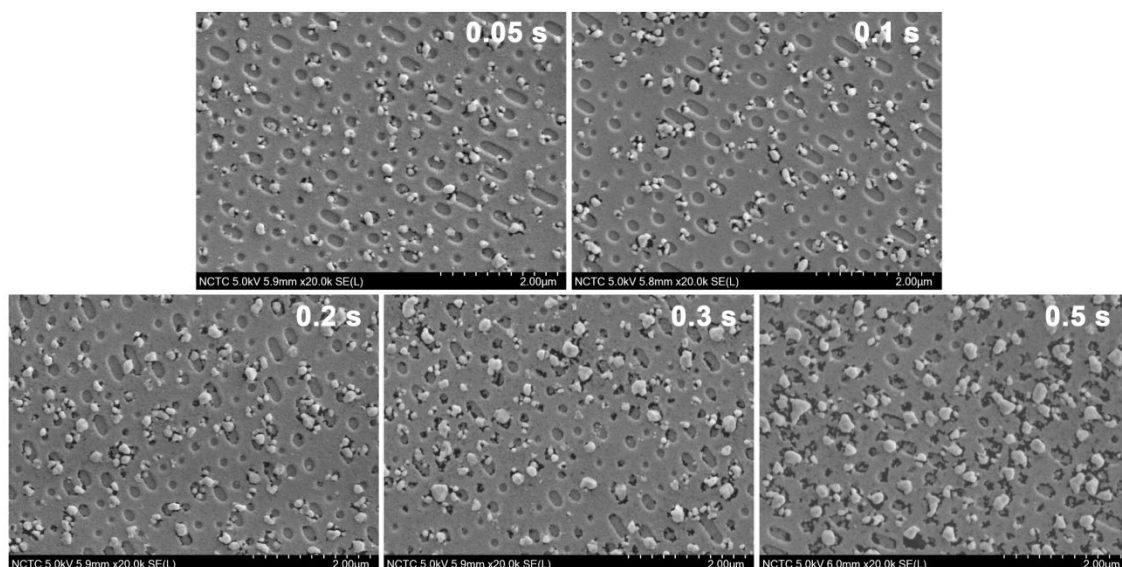


Figure S4. FE-SEM images of r-AgBD-ROM fabricated under different duration time.

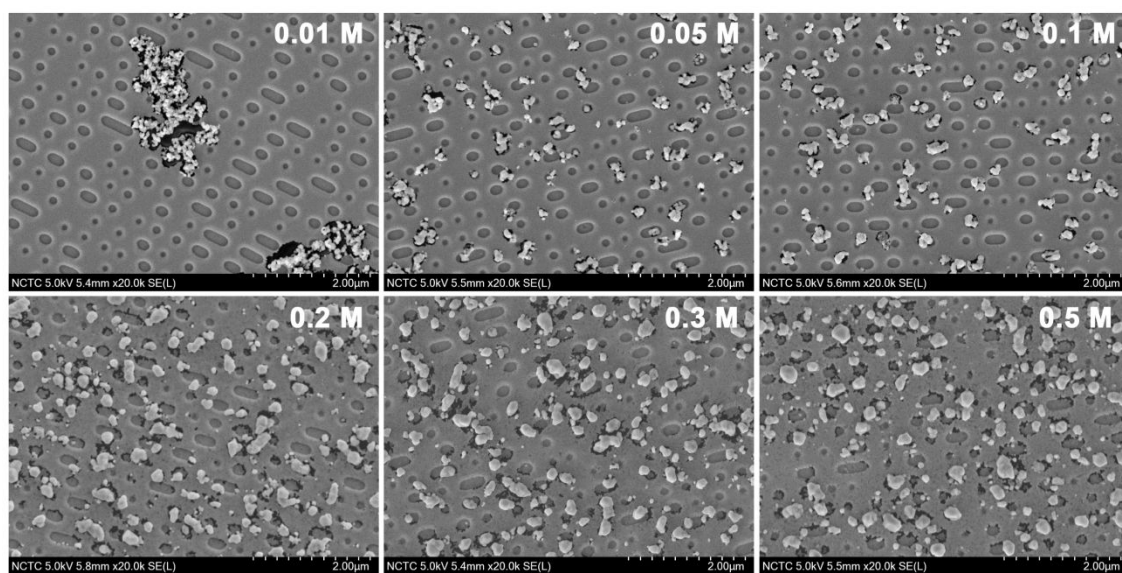


Figure S5. FE-SEM images of r-AgBD-ROM fabricated under different KCl concentrations.

Optimization of Au-r-AgBD-ROM substrate fabrication

The Au-r-AgBD-ROM substrates fabricated under 0, 0.1 and 0.5 mM HAuCl_4 solution were chosen as representative substrates to investigate particle size and size distribution of AgNPs and Au-AgNPs. The histogram of particle size distribution evaluated from 78-91 particles in SEM images ($3 \times 3 \mu\text{m}^2$) using imageJ software is shown in Figure S6. The average particle size and polydispersity index (PDI) were obtained by Gaussian fitting. The average particle size were 50 ± 14.3 , 66.12 ± 30.12 , and 146.62 ± 81.94 nm for Au-r-AgBD-ROM fabricated under 0, 0.1 and 0.5 mM HAuCl_4 solution, respectively. The PDI values were 0.29, 0.46, and 0.56 for Au-r-AgBD-ROM fabricated under 0, 0.1 and 0.5 mM HAuCl_4 solution, respectively.

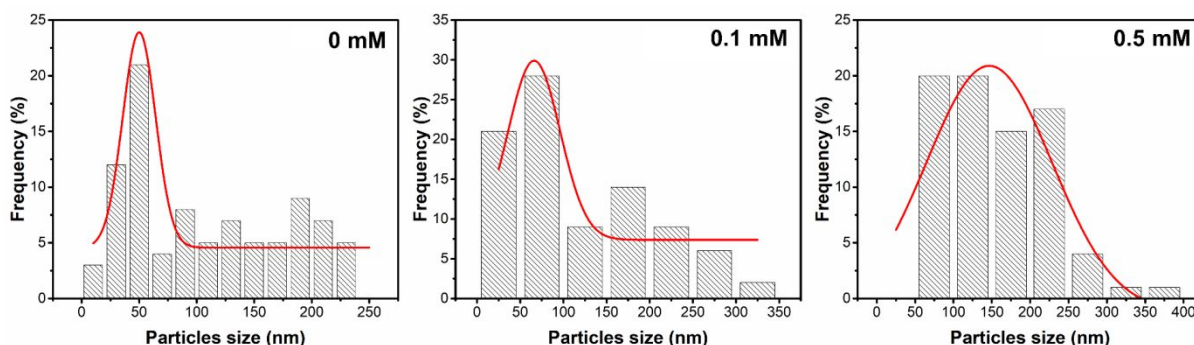


Figure S6. Histogram of NPs size distributions on the Au-r-AgBD-ROM fabricated under 0, 0.1 and 0.5 mM HAuCl_4 solution. The red curves represent a Gaussian fitting.

Elemental composition analysis of SERS substrates during EC treatment and Au coating methods

Table S1 The atomic percentage of elements on the as-prepared substrates obtained from XPS measurements

Peaks	Atomic compositions (%)
-------	-------------------------

	AgBD-ROM	r-AgBD-ROM	Au-r-AgBD-ROM
Ag3d _{3/2} (metal)	16.91	3.42	15.78
Ag3d _{5/2} (metal)	24.98	5.04	23.32
Ag3d _{3/2} (Ag-O-Ag)	-	6.86	4.56
Ag3d _{5/2} (Ag-O-Ag)	-	10.13	6.74
O1s (C-O)	7.13	9.53	5.07
O1s (Ag-O-Ag/O-H/Au-O)	10.64	7.46	2.19
O1s (Absorb with H ₂ O)	-	1.54	2.19
C1s (C-C)	22.82	28.06	22.18
C1s (C-O)	8.34	17.37	8.25
C1s (C=O)	5.59	5.99	3.07
C1s (O=C-O)	3.59	2.43	2.25
C1s (shake-up)	-	2.17	-
Au4f _{5/2} (metal)	-	-	1.51
Au4f _{7/2} (metal)	-	-	2.01
Au4f _{5/2} (Au ⁺)	-	-	0.38
Au4f _{7/2} (Au ⁺)	-	-	0.50

Possible model for SERS enhancement phenomenon

Table S2 Surface roughness (RMS) and surface area of AgBD-ROM and r-AgBD-ROM obtained from AFM measurement.

substrate	RMS	Surface area (nm ²)
AgBD-ROM	2.232	25.008

Surface area reported in Table S2 were calculated from S ratio, which represents the ratio between the real interfacial area and scan area ($5 \times 5 \mu\text{m}^2$).

SERS substrate performance

LOD calculation

The equation used to estimate the limit of detection (LOD) in this study was displayed below.¹

$$LOD = \frac{I_{avg(blank)} + 1.645(SD_{blank} + SD_{low conc}) - b}{a} \quad (S1)$$

Where $I_{avg(blank)}$ and SD_{blank} are the average intensity and the standard deviation of a blank solution (n=10), respectively. $SD_{low conc}$ is the standard deviation of the low concentration sample. a and b are the slope and y-intercept of the sensitivity calibration curve, respectively.

EF calculation

The SERS enhancement factors (EFs) of our SERS substrates were evaluated using methylene blue (MB) as a Raman probe. SERS substrates (r-AgBD-ROM and Au-r-AgBD-ROM) and reference substrate (AgBD-ROM) in the dimension of $1 \times 1 \text{ cm}^2$ were soaked in 1 mL of 10 μM MB aqueous solutions for overnight and dried in an N_2 stream. The standard equation used to calculate EFs in this study was displayed below.²

$$EF = \frac{I_{SERS}/N_{SERS}}{I_{REF}/N_{REF}} \quad (S2)$$

where I_{SERS} and I_{REF} are the average intensities of characteristic Raman peak of MB at 1628 cm^{-1} from SERS and reference substrates, respectively, in the same scattering geometry. N_{SERS} and

N_{REF} are the number of MB molecules absorbed on SERS substrates and reference substrate, respectively. N_{SERS} and N_{REF} were calculated by using the following equations:

$$N_{SERS} \text{ or } N_{REF} = C_{absorb} V_{soak} N_A \quad (S3)$$

$$C_{absorb} = C_{soak} - C_{remain} \quad (S4)$$

where C_{soak} , C_{absorb} and C_{remain} are molar concentrations of MB solution using to soak the substrates (10^{-6} M), absorbed on the substrates and remaining in solution, respectively. V_{soak} is the volume (L) of MB solution using to soak the substrates (10^{-3} L) and N_A is Avogadro's number ($6.02 \times 10^{23} \text{ mol}^{-1}$). C_{remain} was examined from the decrease of UV-VIS absorption intensity of remaining MB aqueous solutions. To calculate C_{remain} , the standard calibration curve of MB in a concentration range of 2 – 10 μM was constructed with UV-VIS absorbance measurements.

The calibration plot constructed from UV-VIS absorbance at 663 nm of MB standard solution (in water) was displayed in Figure S6. C_{remain} was estimated from the linear regression obtained from the calibration curve ($y = 0.0862x + 0.0854$, $R^2 = 0.999$). C_{absorb} , N_{SERS} , and N_{REF} can be calculated using Equation S3 and Equation S4. The calculated parametric values of each substrate were reported in Table S3. N_{SERS} and N_{REF} calculated from Equation S3 are the number of MB molecules absorbed on the entire area of substrate. MB molecules under irradiated area (5 microns in diameter, area = $19.625 \times 10^{-8} \text{ cm}^2$) on the substrate were also estimated as shown in Table S3. Based on the calculations in Equation S1, EFs from r-AgBD-ROM and Au-r-AgBD-ROM are determined to be 3.2×10^3 and 2.1×10^3 , respectively.

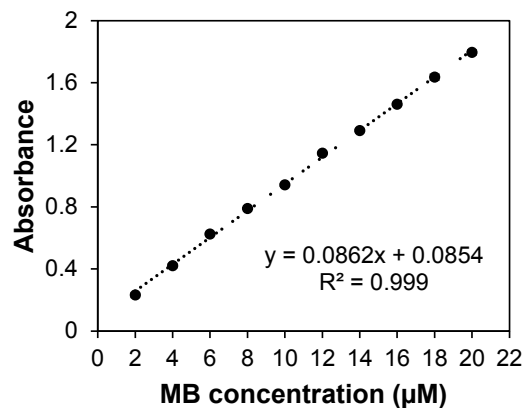


Figure S7. The calibration plot constructed from UV-VIS absorbance at 663 nm of MB standard solution (in water).

Table S3. The calculated parametric values of each substrate.

Substrates			N_{SERS} or N_{REF}	N_{SERS} or N_{REF}	I_{SERS} or I_{REF}
	C_{remain}	C_{absorb}	(molecules)	In scattering	(counts)
	(M)	(M)		area	
				(molecules)	
AgBD-ROM					
(reference substrate)	7.99×10^{-6}	2.01×10^{-6}	1.21×10^{15}	23.74×10^7	10.39
r-AgBD-ROM					
(SERS substrate)	7.86×10^{-6}	2.14×10^{-6}	1.29×10^{15}	25.32×10^7	35940.21
Au-r-AgBD-ROM (SERS substrate)					
	7.66×10^{-6}	2.34×10^{-6}	1.41×10^{15}	27.67×10^7	25425.73

SERS practical application

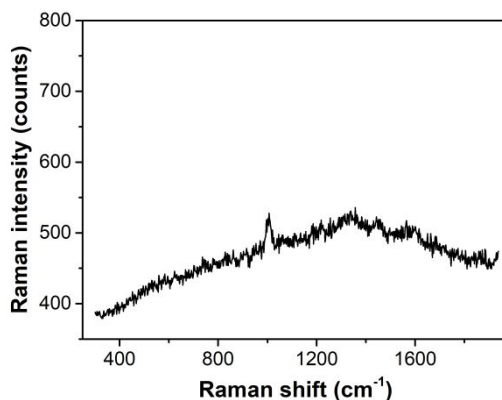


Figure S8. Raman spectra of bare Au-r-AgBD-ROM.

Table S4. Assignments of main peaks for Raman and SERS spectra of acetaminophen recorded on powder state and the Au-r-AgBD-ROM, respectively.

Acetaminophen		
Bulk powder	SERS	Assignments ³
1654		amide I
1613	1618	ν CC (ring)
1562	1567	ν CC, σ^{ip} HNC
1450		σ^{as} CH ₃
1374		σ^{s} CH ₃
1328	1327	amide III band (ν CN/ ν CN (\emptyset)/CNH band)
1260	1275	ν CO, σ^{ip} HCC, ν CC
1241	1244	ν CC, σ^{ip} HOC
1172	1189	σ^{ip} HCC, ν CC
859	859	ν CC (ring)
797		ν CNC (ring)

Table S5. Assignments of main peaks for Raman and SERS spectra of ibuprofen recorded on powder state and the Au-r-AgBD-ROM, respectively.

Ibuprofen		
Bulk powder	SERS	Assignments⁴
1610	1613	ν_{ip} CC _{arom}
1571	1569	ν_{ip} CC _{arom} ν_{as} COOH
1344	1339	ω HCH
1210	1208	τ HCCC _{alif}
1186	1186	τ HCCC _{alif}
1010	1010	δ_{ip} HCC _{arom}
786		δ_{ip} CCOOH
748		δ_{oop} CCOOH
640	644	δ_{oop} CCC _{arom}

Table S6. Assignments of main peaks for Raman and SERS spectra of mefenamic acid recorded on powder state and the Au-r-AgBD-ROM, respectively.

Mefenamic acid		
Bulk powder	SERS	Assignments⁵
1626		β NH, ν CC ($\emptyset 2$), β OH + ν C=O (f)
1605	1605	β NH, ν CC ($\emptyset 1$ and $\emptyset 2$), β OH + ν C=O
1585	1587	β NH (g), ν CC ($\emptyset 1$ and $\emptyset 2$)
1516	1518	ν CC ($\emptyset 2$), β NH (g)
1448		β NH, β CH ($\emptyset 1$ and $\emptyset 2$), δ CH ₃
1408		β NH, ν CC ($\emptyset 1$ and $\emptyset 2$), β OH + ν C=O (e)
1339	1334	β OH (j), ν CC ($\emptyset 2$)
1281	1269	β CH in phase ($\emptyset 1$, $\emptyset 2$), ν CC ($\emptyset 1$), ν C8N, β NH
1248	1246	β OH, β CH in phase ($\emptyset 1$, $\emptyset 2$), ν CCOOH
1165	1162	β CH ($\emptyset 2$)
1097		β CH ($\emptyset 1$, $\emptyset 2$), ω CH ₃

1085	1085	
1044	1025	ν CC ($\emptyset 2$)
994		ω CH ₃
812	817	γ CH in phase ($\emptyset 1$), δ CCC in phase ($\emptyset 2$), β COOH
777	786	γ CH in phase ($\emptyset 1$), β COOH
705	709	CCC in phase puckering ($\emptyset 1$, $\emptyset 2$), γ CH ₃ (C14, C15)
625	623	γ NH (k)
578		δ CCC in phase ($\emptyset 1$, $\emptyset 2$)

Abbreviations: \emptyset = phenyl group, $\emptyset 1$, $\emptyset 2$ = phenyl group labeled according to Figure 8 in main manuscript, ν = stretching, δ = bending, β = bending in plane, γ = bending out of plane, r = rocking, w = wagging, τ = twisting, s = symmetric, as = antisymmetric

REFERENCES

1. Karn-orachai, K.; Sakamoto, K.; Laocharoensuk, R.; Bamrungsap, S.; Songsivilai, S.; Dharakul, T.; Miki, K., Extrinsic surface-enhanced Raman scattering detection of influenza A virus enhanced by two-dimensional gold@silver core-shell nanoparticle arrays. *RSC Advances* **2016**, *6* (100), 97791-97799.
2. Le Ru, E. C.; Blackie, E.; Meyer, M.; Etchegoin, P. G., Surface Enhanced Raman Scattering Enhancement Factors: A Comprehensive Study. *The Journal of Physical Chemistry C* **2007**, *111* (37), 13794-13803.
3. Shende, C.; Smith, W.; Brouillette, C.; Farquharson, S., Drug stability analysis by Raman spectroscopy. *Pharmaceutics* **2014**, *6* (4), 651-62.

4. Di Foggia, M.; Bonora, S.; Tinti, A.; Tugnoli, V., DSC and Raman study of DMPC liposomes in presence of Ibuprofen at different pH. *Journal of Thermal Analysis and Calorimetry* **2016**, *127* (2), 1407-1417.
5. Cunha, V. R.; Izumi, C. M.; Petersen, P. A.; Magalhaes, A.; Temperini, M. L.; Petrilli, H. M.; Constantino, V. R., Mefenamic acid anti-inflammatory drug: probing its polymorphs by vibrational (IR and Raman) and solid-state NMR spectroscopies. *J Phys Chem B* **2014**, *118* (16), 4333-44.